ISSN1027-5495. Functional Materials, 32, No.1 (2025), p. 21-27
doi:http://dx.doi.org/10.15407/fm32.01.21 © 2025 — STC "Institute for Single Crystals"

Absorption of electromagnetic radiation by an ordered composite based on a cubic lattice of metallic nanodimers

L.O. Abramenko[1], V.M. Matiushyn[1], A.V. Korotun[1,2]

[1] National University "Zaporizhzhia Polytechnic" 64 Zhukovsky Str., Zaporizhzhia, 69063, Ukraine,
[2] G.V. Kurdyumov Institute for Metal Physics of National Academy of Sciences of Ukraine,
36 Academician Vernadsky Blvd., Kyiv, 03142, Ukraine

Received July 30, 2024

The optical properties of an ordered nanocomposite based on a cubic lattice of metallic nanodimers are studied. The expressions for the frequency dependencies of the effective dielectric permittivity and magnetic permeability of the nanocomposite taking into account relaxation processes in metallic inclusions are obtained. The fact of the presence of the "blue" shift of the maximum of the imaginary part of the electric polarizability of the elementary cell, caused by collective effects, has been established. The frequency range in which the real parts of the effective permittivities are negative is determined; therefore, the nanocomposite under study is a "left" medium.

Key words: metallic nanodimer, cubic lattice, elementary cell, effective dielectric permittivity and magnetic permeability, electric and magnetic polarizability, "left-handed" material.

Поглинання електромагнітного випромінювання впорядкованим композитом на основі кубічної ґратки металевих нанодимерів. *Л.О. Абраменко, В.М. Матюшин, А.В. Коротун*

Досліджено оптичні властивості впорядкованого нанокомпозиту – кубічної ґратки металевих нанодимерів. Отримано вирази для частотних залежностей ефективних діелектричної та магнітної проникностей нанокомпозиту з урахуванням процесів релаксації в металевих включеннях. Встановлено факт наявності «синього» зсуву максимуму уявної частини електричної поляризуємості елементарної комірки, викликаного колективними ефектами. Визначено частотний інтервал, в якому дійсні частини ефективних проникностей від'ємні, а, отже, досліджуваний нанокомпозит є «лівим» середовищем.

1. Introduction

Natural materials have the limited set of the optical properties, which have recently been extended due to metamaterials. These are the artificial materials with microstructure elements smaller than the wavelength of light; therefore, they behave as homogeneous media with the effective dielectric permittivity and magnetic permeability depending on their composition, size and shape of microstructure elements. The discovery of such extraordinary phenomena as high-frequency magnetism [1], negative refraction [2, 3] and the possibility of creating an ideal lens based on these ideas [4], has led to the fact that metamaterials are in some cases identified with media with the negative refraction. And the advances in transformational optics [5-8] have led to concepts such as optical cloaking using metamaterials [9-11]. Also of interest is a more traditional but technologically interesting approach to meta-

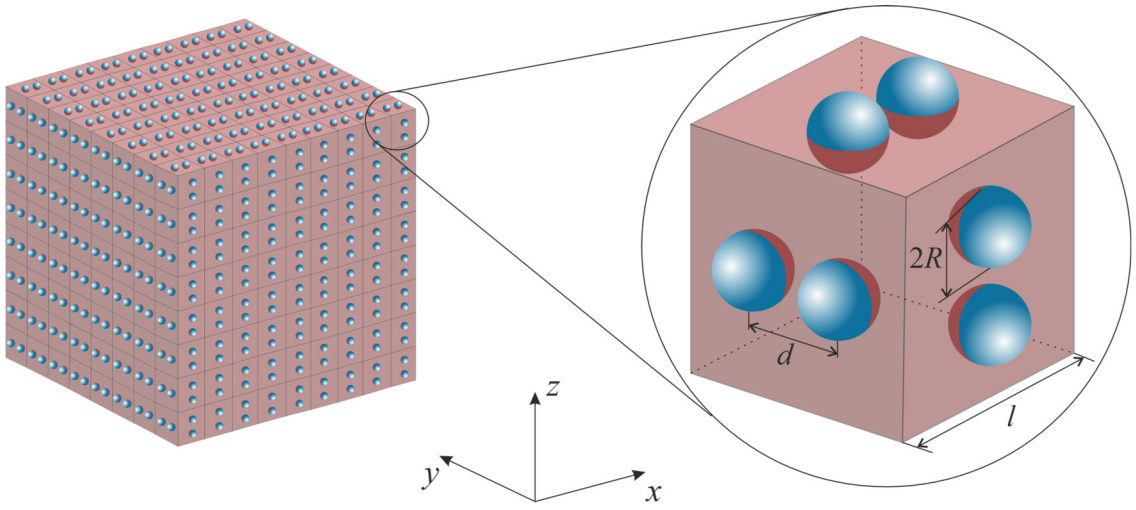

Fig. 1. Ordered nanocomposite and its elementary cell

materials: the ability to obtain an electrical response (typically without magnetic response using nanoparticles tens of nanometers in size as building blocks for synthesizing larger scale structures to control electromagnetic radiation with wavelengths more than 10 times the particle size [12]. The latter can be applied in layers by means of self-assembly, which usually leads to the formation of densely packed structures [13-18]. Such structures have also been widely studied in the search for photonic bandgap materials [19-25].

It should be pointed out that the studies of the effective optical properties of metal-dielectric nanocomposites have a rather long history [26-37]. In the first decades of this research, mainly disordered composites with the low concentration of metallic inclusions were studied and he theory of the effective medium was developed [28, 31, 34]. In recent decades, the issues of creating radio-absorbing coatings ("stealth" technology) [38] and ordered composite media with unique optical properties (in particular, "left-handed" materials) [39, 40] have become relevant.

One of the candidates for "left-handed" materials could be a composite based on the cubic lattice of metallic nanodimers. Therefore, the study of the optical properties of such materials and the determination of the frequency intervals in which they are "left-handed" media is an actual task.

2. Basic relationships

Let us consider an ordered nanocomposite with the properties of the material \ ($\mathrm{Re}\,\epsilon_{\mathrm{eff}}, \mathrm{Re}\,\mu_{\mathrm{eff}} < 0$) consisting of elementary cubic cells, on the faces of which metallic dimers are located (Fig. 1).

The absorption coefficient of such artificial medium is determined by the relation

$$\eta(\omega) = \frac{2\omega}{A\sqrt{\epsilon_{\mathrm{m}}}}\,\mathrm{Im}\sqrt{\epsilon_{\mathrm{eff}}\mu_{\mathrm{eff}}}\,, \qquad (1)$$

where ϵ_{m} is the dielectric permittivity of the matrix, ω and A are the frequency and speed of light.

The effective dielectric permittivity and magnetic permeability

$$\epsilon_{\mathrm{eff}} = \epsilon_{\mathrm{m}}\left(1 + \frac{4\pi n\alpha_{\mathrm{cell}}^{(e)}}{1 - \frac{4\pi}{3}n\alpha_{\mathrm{cell}}^{(e)}}\right); \qquad (2)$$

$$\mu_{\mathrm{eff}} = \mu_{\mathrm{m}}\left(1 + \frac{4\pi n\alpha_{\mathrm{cell}}^{(m)}}{1 - \frac{4\pi}{3}n\alpha_{\mathrm{cell}}^{(m)}}\right), \qquad (3)$$

where $\mu_{\mathrm{m}} = 1$ is the magnetic permeability of the matrix; $n = 1/l^3$ is the number of elementary cells in the unit volume of medium, l is the length of the edge of the elementary cell.

The electric and magnetic polarizabilities of the elementary cell

$$\alpha_{\mathrm{cell}}^{(e)} = 6R^3\left[\frac{\frac{R^3}{\alpha(\omega)} - \frac{1}{\epsilon_{\mathrm{m}}}\left(\frac{R}{d}\right)^3}{\left(\frac{R^3}{\alpha(\omega)} + \frac{1}{\epsilon_{\mathrm{m}}}\left(\frac{R}{d}\right)^3\right)\left(\frac{R^3}{\alpha(\omega)} - \frac{2}{\epsilon_{\mathrm{m}}}\left(\frac{R}{d}\right)^3\right)}\right]; \qquad (4)$$

$$\alpha_{\mathrm{cell}}^{(m)} = \left(\frac{k_0 d}{2}\right)^2 \frac{2R^3}{\frac{R^3}{\alpha(\omega)} - \frac{1}{\epsilon_{\mathrm{m}}}\left(\frac{R}{d}\right)^3}, \qquad (5)$$

Table 1. Parameters of metals (see, for example, [37, 41] and references therein)

Metals / Parameters	Au	Ag	Cu	Pd	Pt
$n_e, 10^{22}$ cm^{-3}	5.91	5.85	17.2	2.53	9.1
ϵ^{∞}	9.84	3.70	12.03	2.52	4.42
$\hbar\omega_p$, eV	9.07	9.17	12.6	9.7	15.2
$\hbar\gamma_{\text{bulk}}$, eV	0.023	0.016	0.024	0.091	0.069
$v_{\text{F}}, 10^6$ m / s	1.41	1.49	1.34	2.84	2.98

Table 2. Dielectric permittivity of various matrices

Parameter	Matrix			
	SiO_2	CaO	CdS	ZnTe
ϵ_{m}	2.1	3.35	5.47	8.76

where R is the radius of a spherical nanoparticle; d is the distance between nanoparticles in a dimer; $k_0 = \omega/c$ is the wavenumber in vacuum; and the polarizability of a nanoparticle in a dimer

$$\alpha(\omega) = R^3 \frac{\epsilon(\omega) - \epsilon_{\text{m}}}{\epsilon(\omega) + 2\epsilon_{\text{m}}}. \quad (6)$$

Dielectric function of a nanoparticle, according to the Drude model

$$\epsilon(\omega) = \epsilon^{\infty} - \frac{\omega_p^2}{\omega(\omega + \text{i}\gamma_{\text{eff}})}, \quad (7)$$

where ω_p is the plasma frequency; ϵ^{∞} is the contribution of the interband transitions into the dielectric function; and the effective relaxation rate

$$\gamma_{\text{eff}} = \gamma_{\text{bulk}} + \gamma_{\text{surf}} + \gamma_{\text{rad}}. \quad (8)$$

In formula (8), bulk relaxation rate $\gamma_{\text{bulk}} = \text{const}$ for the specific material, and the surface relaxation rate and the radiation damping rate [41]

$$\gamma_{\text{s}} = \mathscr{A}(\omega, R)\frac{v_{\text{F}}}{R}; \quad (9)$$

$$\gamma_{\text{rad}} = \left\{\frac{2}{9}\sqrt{\frac{\epsilon^{\infty} + 2\epsilon_{\text{m}}}{\epsilon_{\text{m}}}}\left(\frac{\omega_p R}{c}\right)^3 \mathscr{A}(\omega, R)\frac{v_{\text{F}}}{R}\right\}, \quad (10)$$

where

$$\mathscr{A}(\omega, R) = \frac{3}{4}\frac{1}{\epsilon^{\infty} + 2\epsilon_{\text{m}}}\left(\frac{\omega_p}{\omega}\right)^2 \times \left[1 - \frac{2\nu_s}{\omega}\sin\frac{\omega}{\nu_s} + 2\left(\frac{\nu_s}{\omega}\right)^2\left(1 - \cos\frac{2\nu_s}{\omega}\right)\right], \quad (11)$$

and $\nu_s = v_{\text{F}}/2R$ is the frequency of individual oscillations of electrons.

Thereafter, the relations (1) – (5) taking into account (6) – (11) will be used to obtain the numerical results.

3. Results and Discussion

The optical characteristics of cubic lattices of nanodimers and their elementary cells have been calculated for particles of the different radii and different metals in different matrix media. The parameters of metals and dielectric media for the calculations are given in Tables 1 and 2.

The results of calculating the frequency dependences of the real and imaginary parts and the modulus of electric polarizability for a unit cell with Ag dimers of different sizes in a CaO matrix are given in Fig.2. As in the case of a single silver particle, $\text{Re}\,\alpha_{\text{cell}}^{(e)}$ is an alternating function of frequency, while $\text{Im}\,\alpha_{\text{cell}}^{(e)} > 0$ in the whole frequency range under investigation. However, in the case of a cubic elementary cell with dimers, there is a "blue" shift of $\max\left\{\text{Im}\,\alpha_{\text{cell}}^{(e)}\right\}$ with increasing radius of nanoparticles in the dimer in contrast to single nanoparticles, for which the position of the maximum of the imaginary part of polarizability does not change with the change in their radius. The indicated shift is a manifestation of the collective effects in the cubic elementary cell.

The frequency dependence curves of the real and imaginary parts as well as the modulus of magnetic polarizability for the same unit cell are shown in Fig. 3. It should be noted that the corresponding curves of magnetic

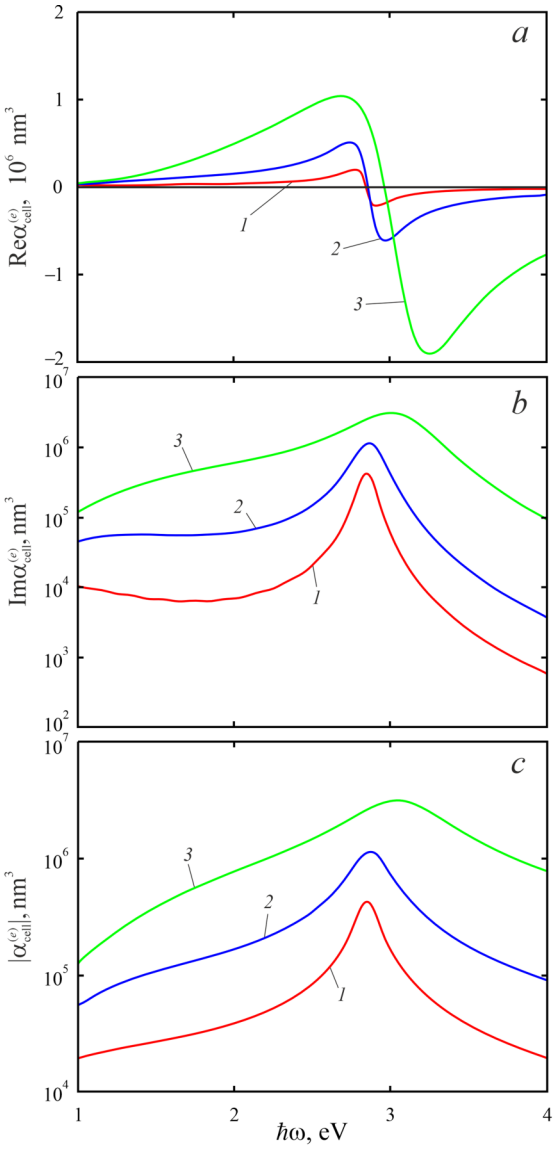

Fig. 2. Frequency dependencies for the real (*a*) and imaginary (*b*) parts, and modulus (*c*) of the electric polarizability for a unit cell with Ag dimers of different sizes in a CaO matrix: *1*– $R = 10$ nm; *2*– $R = 25$ nm; *3*– $R = 50$ nm ($d = 75$ nm; $l = 120$ nm).

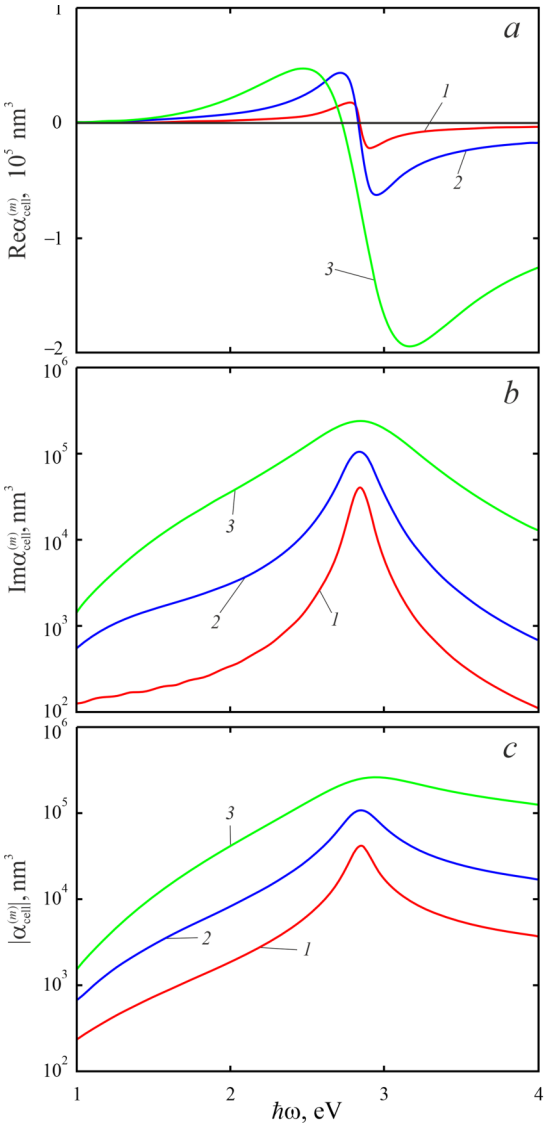

Fig. 3. Frequency dependencies for the real (*a*) and imaginary (*b*) parts, and modulus (*c*) of the magnetic polarizability for a unit cell with Ag dimers of different sizes in a CaO matrix: *1*– $R = 10$ nm; *2*– $R = 25$ nm; *3*– $R = 50$ nm ($d = 75$ nm; $l = 120$ nm).

and electric polarizability are qualitatively similar, but the quantitative differences are significant. Thus, $\max\left\{\mathrm{Re}(\mathrm{Im})\alpha_{\mathrm{cell}}^{(e)}\right\}$ is greater than $\max\left\{\mathrm{Re}(\mathrm{Im})\alpha_{\mathrm{cell}}^{(m)}\right\}$ by one to two orders of magnitude due to the fact that the wave parameter is small ($k_0 d \ll 1$). At the same time there are no shifts of $\max\left\{\mathrm{Im}\,\alpha_{\mathrm{cell}}^{(m)}\right\}$ when changing the radius of nanoparticles in dimers, while $\max\left\{\mathrm{Im}\,\alpha_{\mathrm{cell}}^{(m)}\right\}$ shift towards higher frequencies with an increase in the radius of nanoparticles in dimers.

The frequency dependence curves of the real and imaginary parts of the effective dielectric permittivity and magnetic permeability of the cubic lattice of nanodimers with the different radii of the particles in the dimer are shown in Figures 4 and 5. The medium (composite) is "left-handed" when two conditions are simultaneously fulfilled

$$\begin{cases} \mathrm{Re}\,\epsilon_{\mathrm{eff}} < 0; \\ \mathrm{Re}\,\mu_{\mathrm{eff}} < 0, \end{cases} \qquad (12)$$

Then it is possible to determine the frequency range in which the system of inequalities (12) is valid, which means that the ordered nanocomposite under study is a "left-handed" material. From Fig. 5 it is evident that in the case of particles with relatively small radii ($R = 10, 25$ nm) the studied material based on Ag dimers in CaO will not be "left-handed"

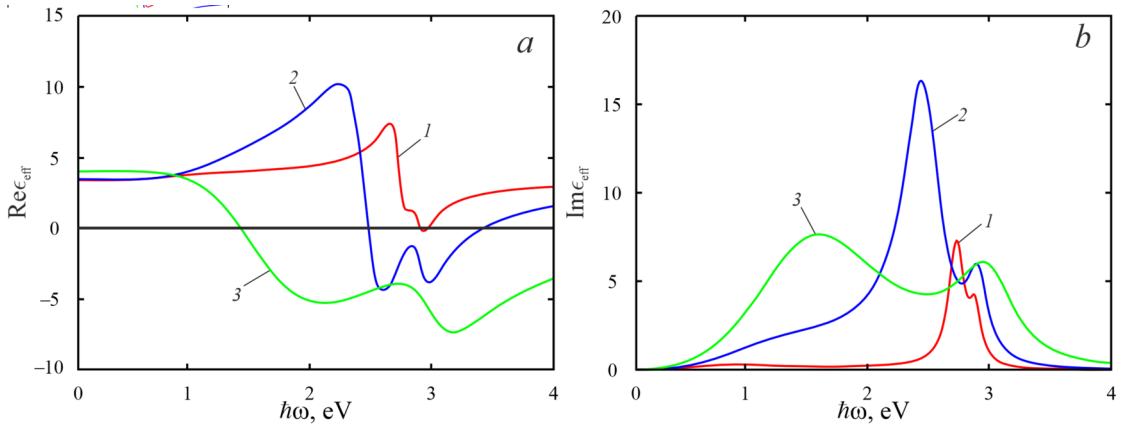

Fig. 4. Frequency dependencies for the real (*a*) and imaginary (*b*) parts of the effective dielectric permittivity of a nanocomposite based on a cubic lattice of Ag dimers of different sizes in a CaO matrix: *1* – $R = 10$ nm ; *2* – $R = 25$ nm ; *3* – $R = 50$ nm ($d = 75$ nm ; $l = 120$ nm).

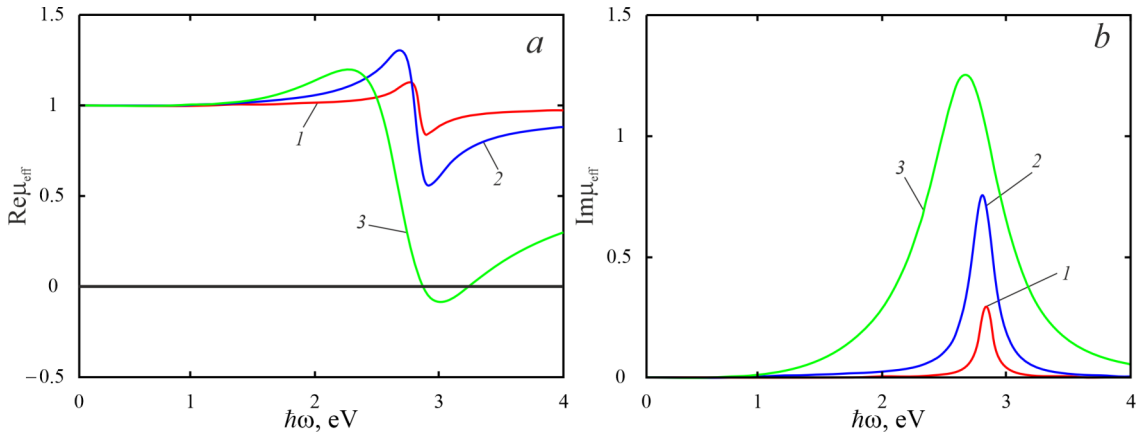

Fig. 5. Frequency dependencies for the real (*a*) and imaginary (*b*) parts of the effective magnetic permeability of a nanocomposite based on a cubic lattice of Ап dimers of the different sizes in a CaO matrix: *1* – $R = 10$ nm ; *2* – $R = 25$ nm ; *3* – $R = 50$ nm ($d = 75$ nm ; $l = 120$ nm).

under any conditionsforanyfrequency $\mathrm{Re}\mu_{eff} > 0$. In turn, if the particles in the dimers have radii $R = 50$ nm , then in a small frequency band (defined by the inequality $\mathrm{Re}\mu_{eff} < 0$, since the inequality $\mathrm{Re}\epsilon_{eff} < 0$ is valid in a sufficiently wide frequency band) such a cubic lattice of nanodimers will exhibit the properties of a "left-handed" material (Fig. 6).

Some other qualitative and quantitative differences in the frequency dependence curves of dielectric permittivity and magnetic permeability of the nanocomposite should also be pointed out. Thus, the values $\left|\mathrm{Re}(\mathrm{Im})\mu_{eff}\right|$ are one order of magnitude less than $\left|\mathrm{Re}(\mathrm{Im})\epsilon_{eff}\right|$ for any frequency in the range under the study. This is due to the fact that the magnetic interaction in the system is much weaker that the electrical one. Moreover, the $\mathrm{Re}\mu_{eff}(\omega)$ and $\mathrm{Im}\mu_{eff}(\omega)$ curves have two extrema (maximum and minimum) and one (maximum), respectively. In turn, the number of extrema $\mathrm{Re}\epsilon_{eff}(\omega)$ and $\mathrm{Im}\epsilon_{eff}(\omega)$ depends essentially on the radius of nanoparticles in the dimer. We consider, that the dependence of the number of maxima $\mathrm{Re}\epsilon_{eff}(\omega, R)$ and $\mathrm{Im}\epsilon_{eff}(\omega, R)$ on the radius of nanoparticles in the dimer is explained by the classical size effect which, from a mathematical point of view, manifests itself in complex dependences of both $\left|\mathrm{Re}(\mathrm{Im})\epsilon_{eff}(\omega)\right|$ and γ_{eff} on the size of nanoparticles. It should also be pointed out that $\mathrm{Im}\epsilon_{eff}$ and $\mathrm{Im}\mu_{eff}$ increase with increasing radius of nanoparticles in the dimer at the same frequencies. The noted facts indicate an increase in the electrical and magnetic interaction between particles in the dimer and between the dimers themselves. In this case, the intensity of the electric interaction is greater than the intensity of the magnetic interaction by an order of magnitude and this ratio is maintained when the size of the particles in the dimer changes.

The frequency dependencies for the absorption coefficient are shown in Fig. 7. The results of the calculations indicate a "red" shift of the absorption coefficient maxima

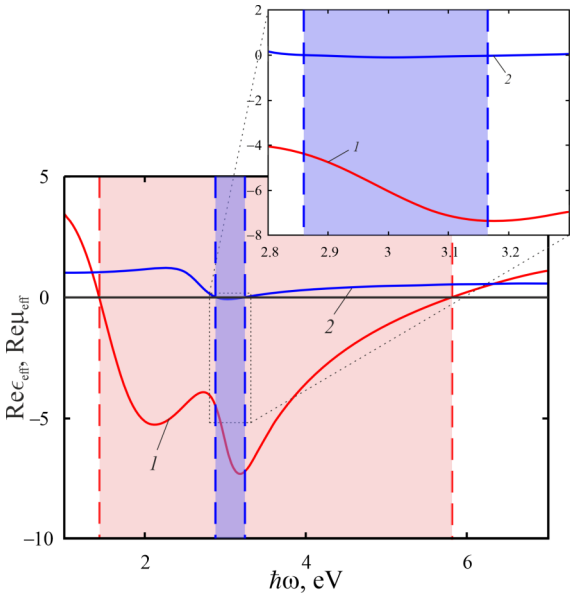

Fig. 6. The frequency region, in which the nanocomposite based on the cubic lattice of Ag dimers with a radius $R = 50$ nm in a CaO matrix has the properties of the "left-handed" material: *1* – $\mathrm{Re}\,\epsilon_{\mathrm{eff}}$; *2* – $\mathrm{Re}\,\mu_{\mathrm{eff}}$ ($d = 75$ nm; $l = 120$ nm).

with a decrease in the radius of nanoparticles in the dimer for metals with lower plasma frequency ($\omega_p^{\mathrm{Au}} < \omega_p^{\mathrm{Ag}} < \omega_p^{\mathrm{Cu}} < \omega_p^{\mathrm{Pd}} < \omega_p^{\mathrm{Pt}}$) and with an increase in the dielectric constant of the matrix medium (in the series of media $\mathrm{SiO_2} \rightarrow \mathrm{CaO} \rightarrow \mathrm{CdS} \rightarrow \mathrm{ZnTe}$).

4. Conclusions

Frequency dependencies for the electric and magnetic polarizabilities of a unit cell, effective dielectric permittivity and magnetic permeability, and absorption coefficient of the composite based on a cubic lattice of metallic dimers have been calculated.

The presence of a "blue" shift in the maximum of the imaginary part of the electric polarizability of the unit cell of the studied composite with an increase in the radius of the particle in the dimer and the absence of a similar shift in the maximum of the imaginary part of the magnetic polarizability were established.

It has been shown that the considered composite can be a "left-handed" material in the certain frequency interval only if the dimers consist of sufficiently large spherical nanoparticles ($R \geq 50$ nm).

The calculation results indicate an increase in the number of extrema of the real and imaginary parts of the effective dielectric permittivity as well as the imaginary parts of the effective dielectric permittivity and magnetic permeability with an increase in the radius of the particles in the dimer due to the strengthening of the electric and magnetic interaction between the particles in the dimer and between dimers themselves.

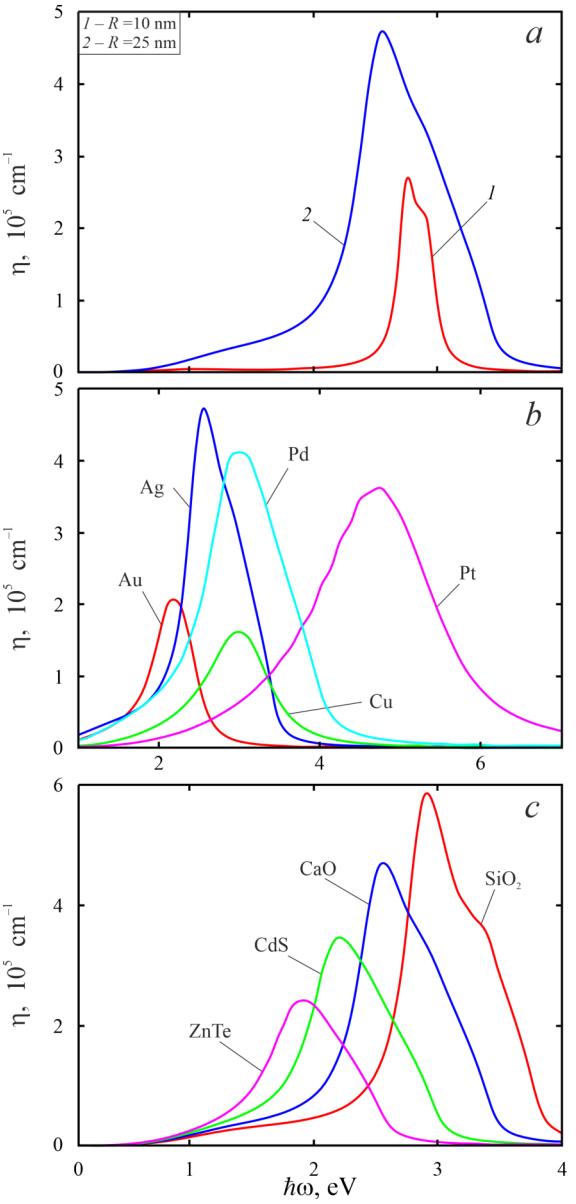

Fig. 7. Frequency dependencies for the absorption coefficient of a nanocomposite based on a lattice of Ag nanodimers of different radii (*a*), nanodimers of different metals in a CaO matrix (*b*), and Ag nanodimers in different matrices (*c*) with $R = 25$ nm ($d = 75$ nm; $l = 120$ nm).

It has been demonstrated that the maxima the frequency dependencies of the absorption coefficient shift to the "red" side with a decrease in the radius of the particles included in the dimer (with a simultaneous increase in the amplitude of the maximum) with a decrease in the plasma frequency (change in the composition of the particles in the dimer), and with an increase in the permittivity of the dielectric matrix.

References.

1. T.J. Yen, W.J. Padilla, N. Fang, D.C. Vier, D.R. Smith, J.B. Pendry, D.N. Basov, X. Zhang, *Science* **303**, 1494-1496, (2004).
2. D.R. Smith, J.B. Pendry, M.C.K. Wiltshire, *Science* **305**, 788-792, (2004).
3. A. Boltasseva, V.M. Shalaev, *Metamaterials* **2**, 1-17, (2008).
4. J.B. Pendry, *Phys. Rev. Lett.* **85**, 3966-3969, (2000).
5. J.B. Pendry, D. Schurig, D.R. Smith, *Science* **312**, 1780-1782, (2006).
6. S. Wang, S. Liu, *Opt Expr* **20**(6), 6777-6787, (2012).
7. S. Wang, X. Liu, Y. Zhu, *Opt Commun* **355**, 80-84, (2015).
8. M.M. Sadeghi, M. Sarisaman, S. Rostamzadeh, *Optics and Laser Technology* **176**, 111036, (2024).
9. D. Schurig, J.J. Mock, B.J. Justice, S.A. Cummer, J.B. Pendry, A.F. Starr, D.R. Smith, *Science*, **314**, 977-980, (2006).
10. W.S. Cai, U.K. Chettiar, A.V. Kildishev, V.M. Shalaev, *Nature Photonics* **1**, 224–227, (2007).
11. Y. Wang, Y. Ge, Z. Zhou, Z.(D). Chen, *Physica Scripta* **99**(8), 085527, (2024).
12. L.M. Liz-Marzán, *Langmuir* **22**, 32-41, (2006).
13. A. Taleb, V. Russier, A. Courty, M.P. Pileni, *Physical Review B* **59**, 13350-13358, (1999).
14. D. Zanchet, M.S. Moreno, D. Ugarte, *Physical Review Letters* **82**, 5277-5280, (1999).
15. M. Gadenne, V. Podolskiy, P. Gadenne, P. Sheng, V.M. Shalaev, *Europhysics Letters* **53**, 364-370, (2001).
16. F. Caruso, M. Spasova, V.S. no Maceira, L.M. Liz-Marzán, *Advanced Materials* **13**, 1090-1094, (2001).
17. T. Ung, L.M. Liz-Marzán, P. Mulvaney, *The Journal of Physical Chemistry B* **105**, 3441-3452, (2001).
18. H. Fan, K. Yang, D.M. Boye, T. Sigmon, K.J. Malloy, H. Xu, G.P. López, C.J. Brinker, *Science* **304**, 567-571, (2004).
19. H. Contopanagos, C.A. Kyriazidou, W.M. Merrill, N. G. Alexópoulos, *Journal of the Optical Society of America A* **16**, 1682-1699, (1999).
20. Z. Wang, C.T. Chan, W. Zhang, N. Ming, P. Sheng, *Physical Review B* **64**, 113108, (2001).
21. A.A. Zakhidov, R.H. Baughman, I.I. Khayrullin, I.A. Udad, M. Kozlov, N. Eradat, V.Z. Vardeny, M. Sigalas, R. Biswas, *Synthetic Metals* **116**, 419-426, (2001).
22. P. Xu, Z. Li, *Journal of Physics D* **37**, 1718-1724, (2004).
23. C.R. Simovski, S.A. Tretyakov, *Physical Review B* **75**, 195111, (2007).
24. Y. Chen, X. Wang, Z. Yong, Y. Zhang, Z. Chen, L. He, P.F. Lee, H.L.W. Chan, C. W. Leung, Y. Wang, *Physics Letters A* **376**(16), 1396-1400, (2012).
25. D. Röhlig, E. Kuhn, F. Teichert, A. Thränhardt, T. Blaudeck, *EPL* **145**(2), 26001 (2024).
26. N.L. Dmitruk, A.V. Goncharenko, E.F. Venger, Optics of small particles and composite media. Naukova Dumka, Kyiv (2009).
27. M. Wang, N. Pan, *Materials Science and Engineering: R: Reports* **63**(1), 1-30, (2008).
28. M.Ya. Sushko, *Journal of Physics D: Applied Physics* **42,** 155410, (2009).
29. S.N. Wani, A.S. Sangani, R. Sureshkumar, *Journal of the Optical Society of America B* **29**, 1443-1455, (2012).
30. C. Etrich, S. Fahr, M.K. Hedayati, F. Faupel, M. Elbahri, C. Rockstuhl, *Materials* **7**(2), 727-741, (2014).
31. V. Markel, *Journal of the Optical Society of America A* **33**(7), 1244-1256, (2016).
32. B.A. Belyaev, V.V. Tyurnev, *Journal of Experimental and Theoretical Physics* **127**(4), 608-619, (2018).
33. A.K. Semenov, *Journal of Physics Communications* **2**, 035045, (2018).
34. S.N. Starostenko, K.N. Rozanov, V. Bovtun, A.O. Shiryaev, *AIP Advances* **10**, 015115, (2020).
35. A.V. Korotun, N.I. Pavlyshche, *Functional Materials* **29**(4), 567-575, (2022).
36. D.T. Meiers, G. von Freymann, *Optics Express* **31**(20), 32067-32081, (2023).
37. A.V. Korotun, N.A. Smyrnova, I.M. Titov, H.M. Shylo, *Metallofiz. Noveishie Tekhnol.* **45**(5), 569-591, (2023) [in Ukrainian].
38. J. Kim, K. Han, J.W. Hahn, *Scientific Reports* **7**(1), 6740 (2017).
39. J. Sancho-Parramon, V. Janicki, H. Zorc, *Optics Express* **18**(26), 26915-26928, (2010).
40. R. Niguma, T. Matsuyama, K. Wada, K. Okamoto, *Photonics* **11**(4), 356, (2024).
41. A.V. Korotun, H.V. Moroz, R.Yu. Korolkov, *Functional Materials* **31**(1), 119-127, 2024.